International Journal of Nanoelectronics and Materials
IJNeaM
ISSN 1985-5761 | E-ISSN 2232-1535

Synthesis of Nano Silicon Using Lasers

Muaath J. Mahmoud 1[a] *, and Bassam G. Rasheed 2[b]

[a]*Laser Research Center, Directorate of Materials Research, Ministry of Science and Technology, Baghdad 10070, Iraq.*
[b]*Laser &Optoelectronics Engineering Department, College of Engineering, Al-Nahrain University, Baghdad 10072, Iraq.*
** Corresponding author. Tel.: +964-770-780-8074; e-mail: muaathjamal@yahoo.com*

Received 5 May 2023, Revised 8 July 2023, Accepted 24 July 2023

ABSTRACT

Two lasers of the same wavelength (1.06 μm) and various specifications were employed to synthesize silicon nanoparticles. The experimental data reveal the formation of stable silicon nanoparticles with different features such as UV-vis absorption, photoluminescence spectrum, Raman spectrum, Zeta potential, and SEM morphology. Theoretical simulations using COMSOL software were adopted to estimate the surface temperature distribution at the silicon surface and underneath. It is found that maximum temperatures of about (5700 K) and (4600 K) were generated when a Q-switched laser pulse of (10 ns) and fiber laser pulse of (127 ns) were used, respectively. While the recoil pressure at the silicon surface was ($6.5*10^5$ N/m2) and ($1*10^3$ N/m2) when Nd:YAG and fiber laser were used respectively. It found that increasing the laser energy for Nd:YAG laser and fiber laser power leads to a blue shift of the absorption spectra while the absorption intensity increases with the number of laser pulses and irradiation time. Raman spectroscopy for the prepared silicon nanoparticles was carried out. The Raman peaks for silicon nanoparticles reveal the formation of amorphous silicon. These peaks were observed at (482) and (475 cm^{-1}) when Nd:YAG and fiber lasers were used to produce those nanoparticles. While the photoluminescence of the prepared silicon nanoparticles exhibits peaks at (457 nm) and (495 nm) for Nd:YAG and fiber lasers. The zeta potential reveals that silicon nanoparticle stability is greater for nanoparticles produced by fiber lasers (27 mv) than those produced by Nd:YAG lasers (17 mv) for three months. The corresponding silicon nanoparticle sizes refer to (3.8 nm) and (6 nm). Potential applications of silicon nanoparticles in optoelectronics and biological imaging can be conducted due to the controllable laser micro/nano machining process.

Keywords: *Silicon nanoparticles, Laser ablation, Silicon nano machining.*

1. INTRODUCTION

The term nanotechnology refers to the design, preparation, and engineering of materials in the range of nanometers [1]. According to the method of synthesis, nanomaterials can be made using either a bottom-up or a top-down approach [2]. The production of nanoscale materials demands precise handling. Nanostructures can have zero, one, two, or three dimensions, and these dimensions can be applied to a wide variety of nanomaterials. Nanomaterials can be synthesized using either chemical or physical processes, depending on the particular type of nanomaterial [3]. Unfortunately, these processes are complicated, and sometimes it is hard to control how pure the product is [4]. The process of using laser ablation to create nanoparticles (NPs) can be divided into two types: dry laser ablation and wet laser ablation [5].

Laser ablation in liquids (LAL) is an excellent way to make nanoparticles because it is easy, quick, and good for the environment. It helps against the chance of contamination in the NPs [6]. Since the synthesis can be done in water or another solution, laser-produced NPs can be more biocompatible, which is necessary for surface functionalization. Silicon nanoparticles can be made without oxidation by using this process [7].

Furthermore, the production of colloidal suspensions of nanoparticles can be accomplished by a process known (PLAL)[8]. The production of nanoparticles with PLAL occurs through a single top-down procedure known as the dispersion approach [9]. One of the most notable benefits of this technology is that it does not require vacuum equipment to produce a wide variety of nanomaterials. These nanomaterials include metals, noble metals, semiconductors, nanoalloys, oxides, and magnetic and core-shell nanostructures. This capacity to produce these nanomaterials is one of the most significant advantages of this technology. Another advantage is the capability of surfactant molecules to control aggregation. However, the use of pulsed lasers is limited in nanotechnology because they frequently produce microparticles [10]. As an alternative to micromachining, laser ablation solids with rapid processing speed and high precision have been widely adopted. The elimination of mass generates a plasma that facilitates the connection of laser energy to the target and increases shock pressure loading. Recent research has examined the potential effects of adding water or other liquids to laser ablation to confine the plasma expansion. According to reports, the containment of plasma expansion by water increases the shock pressure impact [11].

Silicon nanoparticles (NPs) are becoming more attractive because they can be used in many different areas. In

optoelectronic systems, silicon nanoparticles emit red, green, and blue light. Changing the size of nanoparticles can change the range of light they give off. It has been said that silicon nanoparticles have been used successfully as fluorescent agents for both in vivo and in vitro imaging without any noticeable harm. [12]. There are also many studies about the biomedical uses and effects of silicon, as well as nanoparticles made from silicon and toxicology studies. Also, silicon nanoparticles are essential for theorizing about fundamental quantum events. [13].

J. Serrano-Ruz et al. used PLAL to synthesize silicon nanoparticles by applying Nd:YAG laser with a 532 and 1064 nm wavelength, a 6 ns pulse duration, and a 10 Hz pulse rate. Furthermore, they applied the fragmentation process to reduce the size of silicon NPs. They found that using a 1064 nm laser wavelength decreased the size of Si nanoparticles [11]. M. Taheri et al. used PLAL in two stages to synthesize oxide silicon nanoparticles by applying an Nd:YAG laser with a 1064nm wavelength, a 13 ns pulse duration, and a 10 Hz pulse rate. The first stage formed the microstructure. The final stage formed the SiO NPs, which have blue emissions. They show non-toxic syntheses of silicon nanoparticles with an average size of 10 nm [12]. Al-Kattan Ahmed et al. synthesized silicon nanoparticles via PLAL using a femtosecond laser with a wavelength of 1025 nm, a pulse duration of 480 ns, and a pulse rate of 1 KHz. In addition, they utilized fragmentation to reduce Si NPs. Silicon NPs were discovered to have their size reduced from 92 nm to 62 nm with the application of the fragmentation process. [13].

In this work, stable silicon nanoparticles with controllable features are synthesized in PLAL, and theoretical calculations were carried out to estimate the generated heat at the silicon surface and underneath.

2. Experimental methods

An open-mouthed plastic container containing 2.5 ml of deionized water was used to hold a silicon wafer (15.00 mm, 15.00 mm, 0.5 mm) in size. A 1.06 μm Nd:YAG laser was applied for the synthesis process. A laser pulse duration of 10 ns and a repetition rate of (1 Hz) was employed. laser energy density ranging from (2.5 J/cm^2) to (12 J/cm^2) was used for the ablation process. Meanwhile, the fiber laser of the same wavelength, spot size of (100 μm) and output power ranges from (0.3 to 30 W) was also used. The laser energy density of this laser was (0.3-19 J/cm^2). The pulses operate with a repetition rate of (30 kHz) and pulse duration of (127 ns). A five-minute exposure time was used to illuminate the silicon wafer. The PLAL experiment produced a noticeable splash, and clearly visible bubbles followed the laser pulses.

The irradiated area at the silicon surface by the Nd:YAG laser and fiber laser is shown in Figure 1. It is found that the interaction diameter for Nd:YAG laser (1 mm) is greater than that for the fiber laser (200 μm).

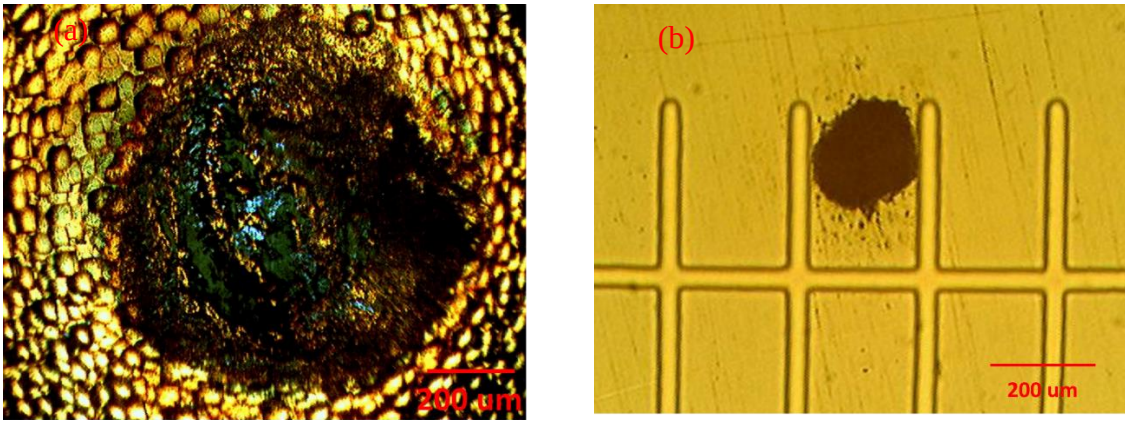

(a) (b)

Figure 1. The optical microscope image of the interaction area for (a) Nd:YAG laser (b) fiber laser.

The interaction area on the Si wafer was observed using a high-resolution optical microscope OLYMPUS BX60M to examine the silicon surface. The optical absorption spectra for a range (300–700 nm) were used by a spectrometer (Model Metrech SP8001). Moreover, photoluminescence measurements were conducted using the FluoroMate FS-2 model spectrometer to calculate the energy gap of silicon nanoparticles. Furthermore, Raman spectroscopy was also adopted to calculate the size of Si NPs.

After that, a portion of silicon nanosuspension was dropped onto glass substrates and allowed to dry at room temperature in a clean environment. The dried suspension on a glass substrate was utilized for SEM (model Inspect S50, FEI-Netherlands) and EDX analysis.

Finally, the residual colloidal solution was then transferred into a quartz tube to examine the stability of NPs using a zeta potential analyzer (Brookhaven, USA).

3. Results and discussion

The prepared silicon nanoparticles were extensively investigated using experimental analysis and theoretical calculations.

3.1. The Experimental Results

- The Optical Properties

The laser wavelength of (1064 nm) was used since this wavelength is highly absorbed by the silicon wafer. The absorption spectra were shown in Figure 2 by UV-visible spectrophotometer for the Si sample irradiated by the Nd:YAG laser and fiber laser.

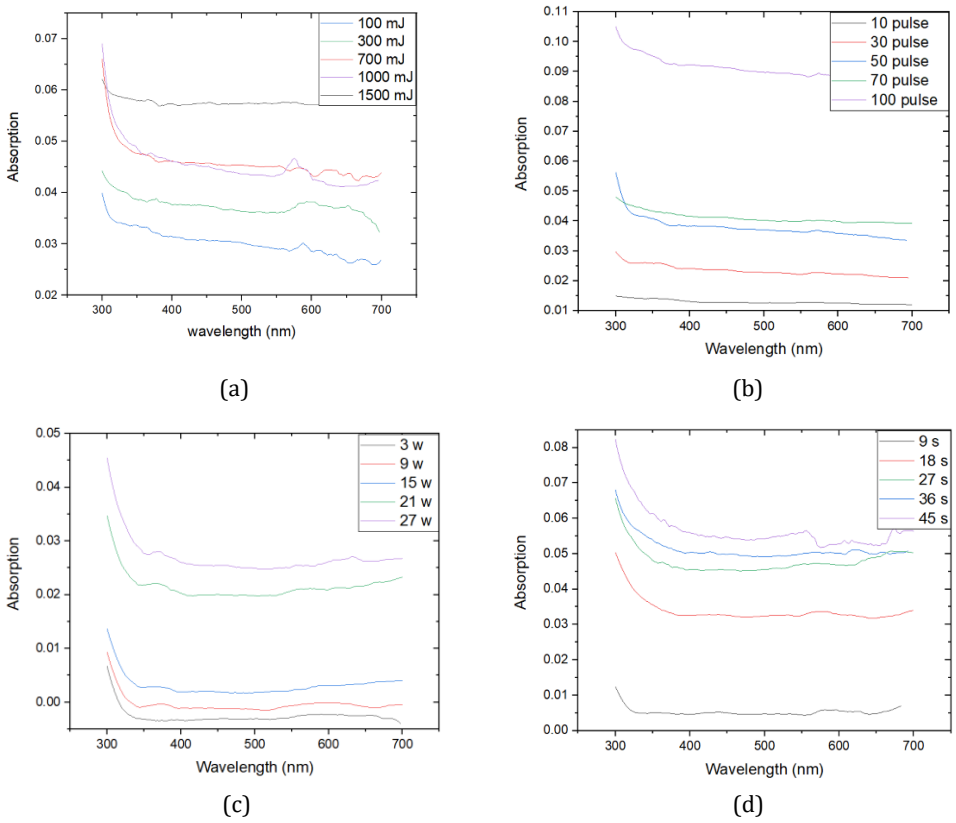

Figure 2. Absorption spectra Si NPs suspension by Nd:YAG laser and fiber laser respectively, (a)Nd:YAG laser with different laser energy,(b) Nd:YAG laser with different a laser pulse,(c) fiber laser with a different laser power,(d) fiber laser with different irradiation time.

Figure 2(a,c) shows that when the laser energy or power increases, the absorption peak is shifted to a higher wavelength. This red-shifted peak indicates that larger NPs were prepared at a higher energy density. Furthermore, Figure 2(b,d) shows that when increasing the laser number of pulses, the peak nearly remains constant, which means that the laser pulse affects the nanoparticles' density only. On the other hand, the photoluminescence of Si NPs suspension produced by an Nd:YAG laser and a fiber laser is shown in Figure 3.

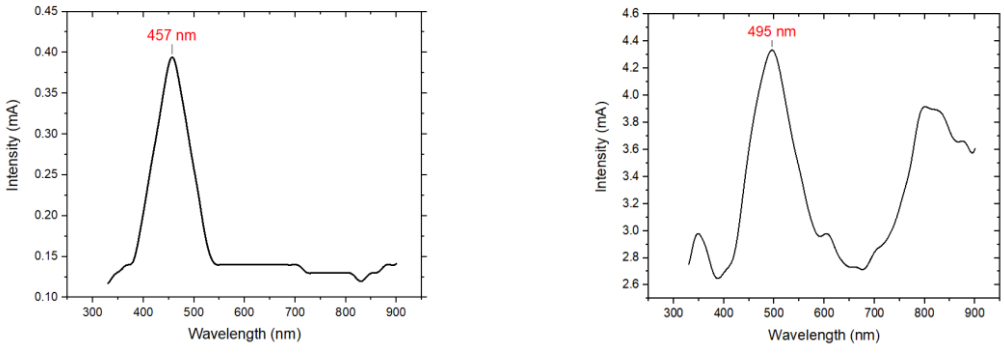

Figure 3. PL spectrum of Si NPs prepared by: (a) Nd:YAG laser and (b) fiber laser.

According to these figures, the energy gap for silicon nanoparticles is (2.6 eV) and (2.5 eV) produced by Nd:YAG and fiber lasers, respectively. Silicon nanoparticle sizes can be estimated using the quantum confinement model, which is given in equation (1) [14].

$$E_{nx,ny,nz} = \frac{\hbar^2\pi^2}{2m}\left[\left(\frac{n_x}{L_x}\right)^2 + \left(\frac{n_y}{L_y}\right)^2 + \left(\frac{n_z}{L_z}\right)^2\right] \quad (1)$$

Where E is energy gap, $\hbar$ is blank constant over 2π, m is effective mass, n is refractive index, L is NPs size.

It is found that the Nd:YAG laser produces smaller nanoparticle sizes (3.8 nm) compared with those produced by the fiber laser (6 nm). That is due to the higher power density of the Nd:YAG laser ($3*10^8$ W/cm^2) which leads to generating a greater temperature and splashing smaller nanoparticles.

The Raman spectrum of Si NPs suspension that was irradiated by the Nd:YAG laser and fiber laser is shown in Figure 4.

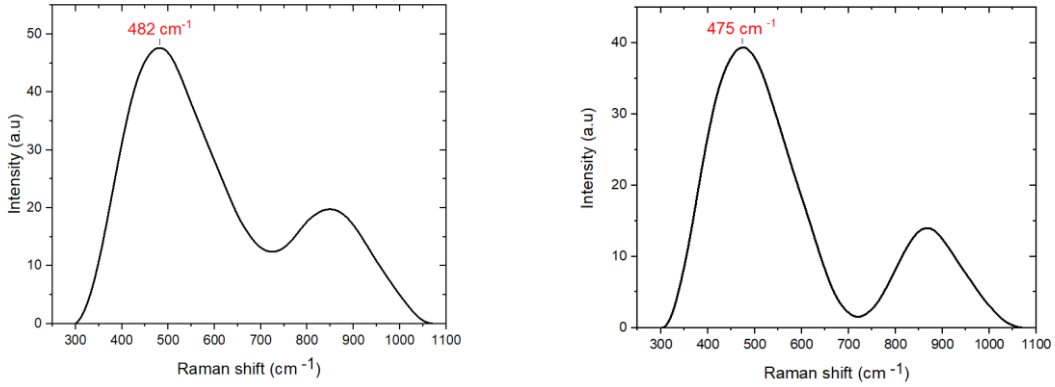

(a) (b)

Figure 4. Raman spectrum of Si NPs prepared by: (a) Nd:YAG laser (b) fiber laser.

The Raman peak positions at (482 cm^{-1}and 475 cm^{-1})for silicon NPs produced by Nd:YAG and fiber laser, respectively, indicate the formation of amorphous silicon nanofilm.

- **The morphological characteristics**

Figure 5 shows the synthesis of different shapes and sizes of silicon nanoparticles by Nd:YAG and fiber laser. The SEM micrographs show the formation of different nanoparticle sizes for dried suspensions above the glass substrate. Because the Nd:YAG laser has a higher energy density, which generates a higher temperature and vapor pressure, it leads to silicon nanoparticles with smaller sizes and a more spherical shape than fiber laser, which agrees with the results in Ref. [2].

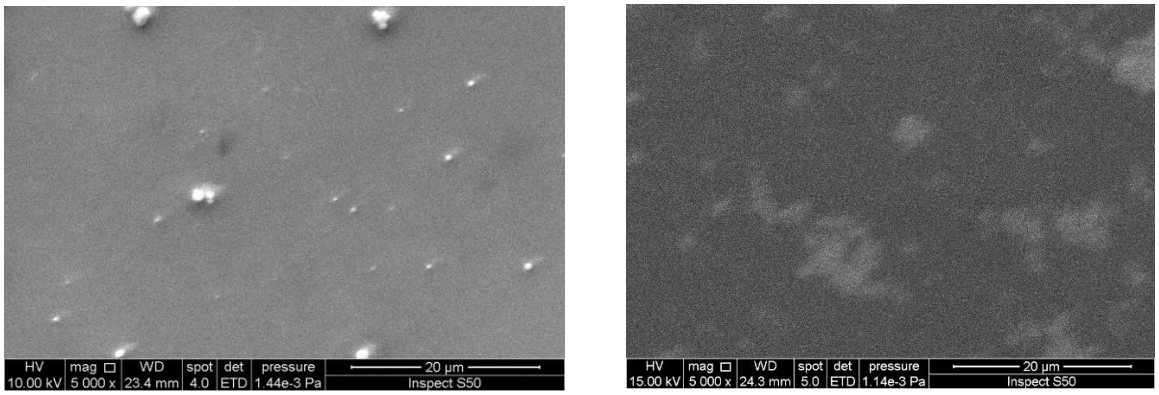

(a) (b)

Figure 5. SEM images of Si NPs prepared by: (a) Nd:YAG laser (b) fiber laser.

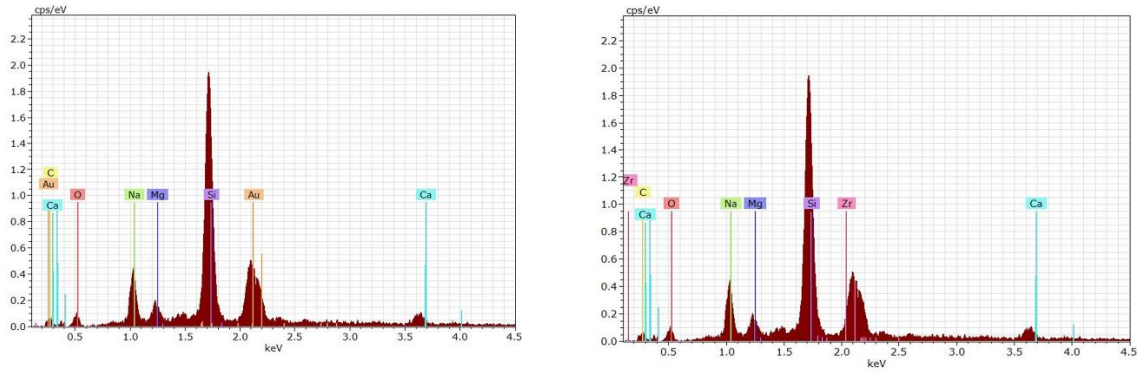

(a) (b)

Figure 6. EDX spectrum of Si NPs prepared by: (a) Nd:YAG laser (b) fiber laser.

Figure 6 reveals the compositions of the elements for the dried suspension above the glass substrate and the glass substrate itself. The EDX chart shows silicon nanoparticles' formation as the primary element in the suspension by Nd:YAG and fiber laser. Moreover, the EDX chart detects some residual elements with very low concentrations, which are the composition of the glass substrate.

- **The stability of silicon nanoparticles**

The stability of the colloidal suspension of silicon nanoparticles produced by both lasers was examined using zeta potential measurements for more than three months. Table 1 indicates the formation of stable nanoparticles, and this stability decreases with time due to the aggregation of NPs, which agrees with Ref. [15].

Table 1. The stability of Si NPs prepared by: (a) Nd:YAG laser (b) fiber laser.

Time	Zeta Potential (mV)	
	Nd:YAG	Fiber
fresh	25.53	35.35
2 week	22.37	33.55
1 month	19.08	31.33
3 month	17.79	27.28

It's also observed that silicon nanoparticles produced by fiber laser have almost higher stability compared with those prepared by Nd:YAG laser. This observation can be explained by the formation of larger NPs with lower aggregation produced by fiber lasers.

3.2. The theoretical calculations

When the laser irradiates the silicon target, its energy is absorbed on the surface, resulting in surface melting, vaporization, and ionization, where the temperatures for Si melting and vaporization were (1687 K) and (3538 K), respectively [15]. During the duration of the pulse, a plasma plume of silicon atoms is formed over the laser interaction spot on the target. This plume has a high temperature, intensity, and pressure. The generation of this plume is followed by the production of a shock wave in the opposite direction, which is caused by the adiabatic expansion of the plume at a supersonic velocity caused by the absorption of the subsequent laser pulse. Then, the plume will grow and lead to a rapid decrease in temperature [16].

In other words, when the laser beam is delivered to the Si surface, the Si surface temperate is increased rapidly due to the high energy density of the laser in a very short time. The surface temperature is given by equation (2) [16]:

$$T=\alpha F.A.(1/pc_n) \quad (2)$$

Where α is absorption coefficient, F is energy density, A is absorptivity, p is density, cp is specific heat. Therefore, when increasing the laser energy, the Si surface temperature increases too, as given in Table 2.

Table 2. Silicon surface temperature(T) as a function of laser energy(E) and laser power(P).

Nd:YAG laser		Fiber laser	
E(J)	T(K)	P(w)	T(K)
0.1	569	5	833
0.2	1137	10	1666
0.4	2275	15	2500
0.6	3411	20	3332
0.8	4548	25	4165
1	5685	30	4997

At the same time, due to the appearance of a plasma plume over the laser spot on the target surface, recoil pressure appeared at the silicon surface. This pressure is given by equation (3) [17]:

$$P=P_0.1.69/\sqrt{L}.\sqrt{KT/mL}/1+2.2(KT/mL)^2 \quad (3)$$

Where Po is power density, L is latent heat, K, thermal conductivity, m is mass of vapor, t is surface temperature. The recoil pressure was ($6.5*10^5$ N/m^2) and ($1*10^3$ N/m^2) when the Nd:YAG laser and fiber laser were used,respectively.

The theoretical model for laser/silicon interaction was designed using COMSOL software. The model is used to simulate the heat distribution at the Si surface and underneath during the interaction process, as shown in Figure 7.

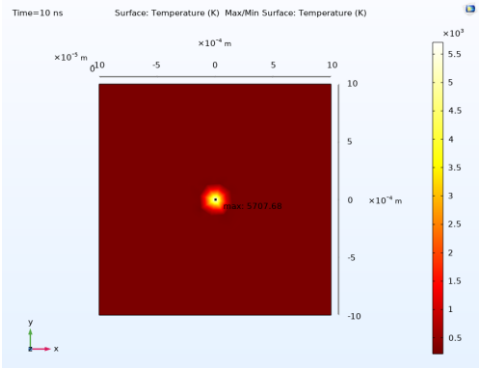

(a)

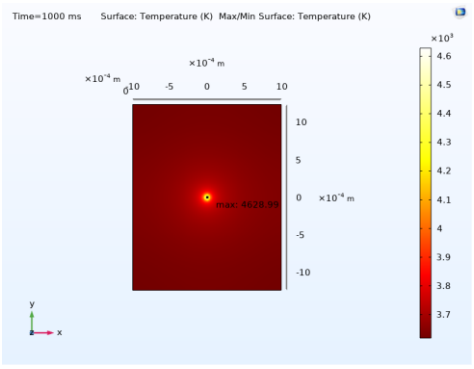

(b)

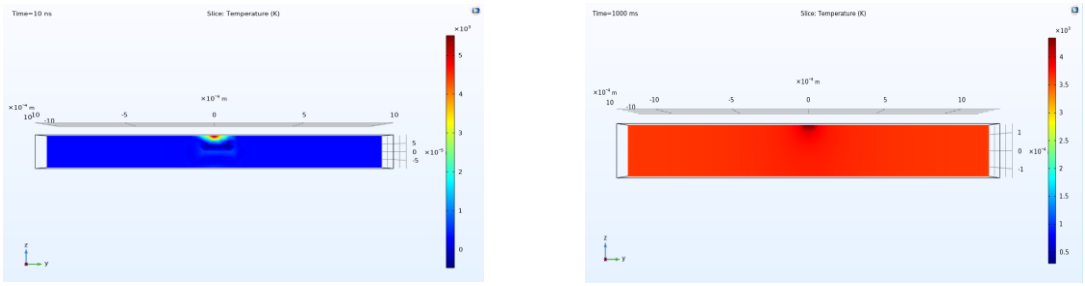

(c) (d)

Figure 7. The theoretical model of: (a) and (b) temperature distribution of Si irradiated by Nd:YAG laser and fiber laser respectively. While (c) and (d) represent the heat penetration in Si by Nd:YAG laser and fiber laser respectively.

Table 3. Silicon surface temperature as a function of irradiation time.

Nd:YAG laser		Fiber laser	
Irradiation Time(ns)	T_{max}(K)	Irradiation Time(s)	T_{max}(K)
1	835	0.1	1828
2	1377	0.2	2368
3	1919	0.3	2883
4	2460	0.4	3351
5	3002	0.5	3749
6	3544	0.6	4060
7	4049	0.7	4290
8	4626	0.8	4453
9	5166	0.9	4540
10	5700	1	4600

Figure 7 shows the temperature distribution of Si for Nd:YAG laser and fiber laser. The maximum surface temperature for the Nd:YAG laser is approximately (5700 K) at (10 ns), whereas the maximum surface temperature for the fiber laser is (4600 K) at (1 s), which is due to the lower laser power density for the fiber laser being less than four orders of magnitude less than that of the Nd:YAG laser, as shown in Figure 7(a,c). The long irradiation time of the fiber laser led to heating all the Si surface and underneath, as shown in Figure 7(b,d). The relation between the surface temperature and the irradiation time for both the Nd:YAG laser and the fiber laser is given in Table 3.

4. Conclusions

Silicon nanoparticles were created by PLAL using 1064 nm Nd:YAG lasers and fiber lasers of different specifications: spot size, energy density, pulse duration, and irradiation time. Larger nanoparticles were produced by lower laser energy densities and larger spot sizes. However, the density of NPs increases with the irradiation time. The theoretical calculations indicate that the laser ablation process raises the surface temperature to a higher value when the Nd:YAG laser is employed. Moreover, greater recoil pressure was established when the Nd:YAG laser was used to prepare silicon nanoparticles. The photoluminescence of silicon nanoparticles reveals the formation of smaller nanoparticles for the Nd:YAG laser compared with fiber lasers. The prepared silicon nanoparticles were found to be stable for a duration longer than three months, and they were more stable those produced by fiber laser.

ACKNOWLEDGMENTS

This work was done at the Laser and Optoelectronics Engineering department, College of Engineering, Al-Nahrain University, Iraq, as a partial requirement of an PHD degree in laser and optoelectronics engineering.

REFERENCES

[1] H. Kobayashi, P. Chewchinda, H. Ohtani, O. Odawara, and H. Wada, "Effects of laser energy density on silicon nanoparticles produced using laser ablation in liquid," *J. Phys. Conf. Ser.*, vol. 441, no. 1, pp. 1–6, 2013

[2] M. S. Hassan, Z. A. Taha, and B. G. Rasheed, "Synthesis and Modeling of Temperature Distribution for Nanoparticles Produced Using Nd:YAG Lasers," *J. Nanotechnol.*, vol. 24, no. 5, pp. 1–8, 2016

[3] M. B. Larosi, V. Garc, and A. Riveiro, "Laser Synthesis of Nanomaterials," *nanomaterials*, vol. 12, pp. 10–13, 2022

[4] D. M. Popovic, J. S. Chai, A. A. Zekic, M. Trtica, J. Stasic, and M. Z. Sarvan, "The influence of applying the additional continuous laser on the synthesis of silicon-based nanoparticles by picosecond laser ablation in liquid," *Laser Phys. Lett.*, vol. 11, no. 6, pp. 1–6, Nov. 2014

[5] T. Feng, G. Chen, H. Han, and J. Qiao, "Femtosecond-Laser-Ablation Dynamics in Silicon Revealed by Transient Reflectivity Change," *micromachines*, vol. 13, no. 14, pp. 1–10, 2022.

[6] K. S. Khashan, R. A. Ismail, and R. O. Mahdi, "Synthesis of SiC nanoparticles by SHG 532 nm Nd:YAG laser ablation of silicon in ethanol," *Appl. Phys. A Mater. Sci. Process.*, vol. 124, no. 6, pp. 1–11, 2018.

[7] D. J. Lim, H. Ki, and J. Mazumder, "Mass removal modes in the laser ablation of silicon by a Q-switched diode-pumped solid-state laser (DPSSL)," *J.*

Phys. D. Appl. Phys., vol. 39, no. 12, pp. 2624–2635, 2006.

[8] B. S. Yuan, Y. Zhang, W. Zhang, Y. Dong, and G. Y. Jin, "The effect of spot size combination mode on ablation morphology of aluminum alloy by millisecond-nanosecond combined-pulse laser," *Materials (Basel)*, vol. 11, no. 8, pp. 1–11, 2018.

[9] W. A. Ghaly and H. T. Mohsen, "Laser-induced silicon nanocolumns by ablation technique," *J. Radiat. Res. Appl. Sci.*, vol. 13, no. 1, pp. 398–405, Jan. 2020.

[10] R. Intartaglia, K. Bagga, M. Scotto, A. Diaspro, and F. Brandi, "Luminescent silicon nanoparticles prepared by ultra short pulsed laser ablation in liquid for imaging applications," *Opt. Mater. Express*, vol. 2, no. 5, pp. 510–518, 2012.

[11] J. A. Serrano-Ruz et al., "Synthesis of silicon nanoparticles by laser ablation at low fluences in water and ethanol," *Mater. Res. Express*, vol. 7, no. 2, pp. 1–9, 2020.

[12] M. Taheri and N. Mansour, "Silicon Nanoparticles Produced by Two-Step Nanosecond Pulsed Laser Ablation in Ethanol for Enhanced Blue Emission Properties," *Silicon*, vol. 12, no. 4, pp. 789–797, 2020.

[13] A. Al-Kattan, L. M. A. Ali, M. Daurat, E. Mattana, and M. Gary-Bobo, "Biological assessment of laser-synthesized silicon nanoparticles effect in two-photon photodynamic therapy on breast cancer MCF-7 cells," *Nanomaterials*, vol. 10, no. 8, pp. 1–11, 2020.

[14] R. Gill, M. Zayats, and I. Willner, "Semiconductor quantum dots for bioanalysis," *Biosensors*, vol. 47, no. 40, pp. 7602–7625, 2008.

[15] H. T. Phan and A. J. Haes, "What Does Nanoparticle Stability Mean?," vol. 123, no. 27, 2019.

[16] W. R. Runyan, *Silicon Semiconductor Technology*, First edition. New York: McGraw-Hill, 1965.

[17] P. Chewchinda, T. Tsuge, H. Funakubo, O. Odawara, and H. Wada. "Laser wavelength effect on size and morphology of silicon nanoparticles prepared by laser ablation in liquid." *Jpn. J. Appl. Phys.*, vol. 52, no. 2, pp. 1–4, Feb. 2013.

[18] H. D. Vora, S. Santhanakrishnan, S. P. Harimkar, S. K. S. Boetcher, and N. B. Dahotre. "One-dimensional multipulse laser machining of structural alumina: Evolution of surface topography." *Int. J. Adv. Manuf. Technol.*, vol. 68, no. 4, pp. 69–83, 2013